Original Paper

Mid-infrared laser absorption spectroscopy for process and emission control in the glass melting industry

Part 2. Difference frequency generation based MIR laser spectrometer for glass melting furnaces

Lothar Wondraczek, Gerhard Heide and Günther Heinz Frischat

Institut für Nichtmetallische Werkstoffe, Technische Universität Clausthal, Clausthal-Zellerfeld (Germany)

Alireza Khorsandi, Ulrike Willer and Wolfgang Schade

Institut für Physik und Physikalische Technologien, Technische Universität Clausthal, Clausthal-Zellerfeld (Germany)

Emerging techniques of mid-infrared absorption spectroscopy offer potentially great sensitivity and selectivity for combustion control and emission monitoring. Because of that, a difference frequency based mid-infrared absorption spectrometer has been considered for application in the glass industry.

Based on preliminary tests within laboratory conditions, a spectrometer which operates at wavelengths around 5 µm was applied to online monitoring of the atmosphere of a gas fired glass melting furnace. The CO concentration was measured in order to demonstrate the feasibility of a mid-infrared absorption spectrometer for process control in the glass industry. A series of measurements was performed in situ as well as crossing the recuperator entry, resulting in general advice on the construction of a prototype device.

1. Introduction

Fundamental aspects and techniques of coherent mid-infrared (MIR) absorption spectroscopy were subject of the first part of the present paper [1]. Since one of the most promising ways to generate coherent MIR radiation for spectroscopic purposes turned out to be difference frequency generation (DFG), a DFG based MIR spectrometer was considered for in situ emission monitoring in the glass industry [2].

The principles of parametric frequency conversion and, in particular, DFG are described elsewhere [3 and 4]. Therefore, just some short comments will be given here. While in classical optics, a linear correlation between polarization $P(t)$ and electro-magnetic field strength $E(t)$ is assumed (equation 1), at higher field strengths nonlinear influences can be observed (equation 2).

$$P_{\text{linear}}(t) = \varepsilon_0 \cdot \chi^{(1)} \cdot E(t), \tag{1}$$

$$P(t) = \varepsilon_0 \cdot \chi^{(1)} \cdot E(t) + \varepsilon_0 \cdot \chi^{(2)} \cdot E^2(t) + \varepsilon_0 \cdot \chi^{(3)} \cdot E^3(t) + \ldots \tag{2}$$

with time t, permittivity ε_0, and n^{th}-order tensor of the susceptibility $\chi^{(n)}$.

Received 16 February 2004.

This results in intensity dependent refractive indices and multi-wave interactions that deviate from the principle of superposition. In solids, the magnitude of susceptibilities are $|\chi^{(1)}| \approx 1$, $|\chi^{(2)}| \approx 10^{-10}$ cm/V and $|\chi^{(3)}| \approx 10^{-17}$ cm^2/V^2. Corresponding to the order of occurring nonlinearities, effects are classified by second, third and higher order. Second order nonlinear effects are two- and three-photon interactions such as DFG, sum frequency generation, optical parametric generation and second harmonic generation, while third order effects are, for example, self-modulation, self-focussing or four-photon interaction. DFG occurs when the interaction of two input waves results in a third wave which oscillates at the difference frequency of the first two. By convention, it is $\lambda_{\text{Pump}} < \lambda_{\text{Signal}} < \lambda_{\text{Idler}}$ where λ_{Pump} is the wavelength of the pumpwave, λ_{Signal} that of the signal wave, and λ_{Idler} that of the idler (in the present case MIR) wave.

The intensity of the generated MIR DFG radiation is given by equation (3) [5]:

$$I_{\text{Idler}} = I_{\text{Pump}} \cdot I_{\text{Signal}} \cdot \psi \cdot L \cdot \sin c^2(|\Delta k| \cdot L/2) \tag{3}$$

where $I_{\text{Pump/Signal/Idler}}$ are the pump, signal, and idler intensity, respectively, L is the interaction (crystal) length, ψ is the frequency conversion efficiency and Δk is the phase mismatch of the interacting waves. While interaction length and conversion efficiency are default parameters, the generated

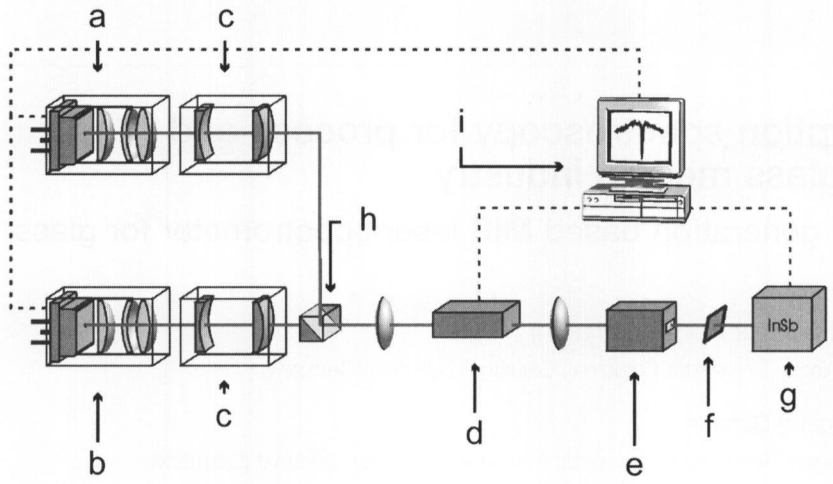

Figure 1. Schematic view of the applied spectrometer (a, b: NIR diode lasers with collimation optics, c: anamorphic optics, d: $AgGaS_2$ crystal, e: gas volume, f: filter, g: detector, h: beam splitter, i: data evaluation); —— laser beam, ----- signal processing.

intensity is strongly dependent on input intensities and optimal phase matching. Thereby, phase matching is crucial.

Because of the optical dispersion of the applied nonlinear optical (NLO) material, inside the material signal, pump and idler wave propagate at different speed. To achieve optimal overlapping of all three waves and, thus, optimal interaction, propagation speed and refractive indices, respectively, have to be properly adjusted. Phase matching can be achieved by using the natural birefringence of the material (BPM). Parameters influencing the refractive index are the crystal temperature and the angle of incidence. For critical BPM, the angle of incidence is properly adjusted while for noncritical BPM, normal incidence is used. In type I BPM, signal and idler are equally polarized while in type II BPM their polarization is different. A second possibility is quasi phase matching (QPM) in periodically structured materials. Phase matching is then achieved by proper engineering of the modulating structures [6]. In the present investigation, noncritical type I BPM in $AgGaS_2$ is applied. It has been investigated in detail by Willer et al. in [7].

2. Experimental

Within the scope of preliminary investigations under laboratory conditions, the applied spectrometer was optimized for industrial application. Some results are given in [8]. Online absorption experiments were perfomed at the gas/air fired 12 t/d FlexMelter® aggregate of Dr. Genthe GmbH & Co. KG, Goslar (Germany).

2.1 Mid-infrared laser source

The experimental setup of the MIR DFG spectrometer is shown in figure 1 and described in detail elsewhere [7 to 9]. Two continuous wave (cw) single mode diode lasers (Toshiba TOLD 9150 and Sharp LT024MDO) are used as pump and signal lasers. By accurate temperature and current control, the diodes can be tuned from 680 to 682 and from 787 to 791 nm, respectively. Elliptical beam profiles of the near-infrared diodes were transformed to Gaussian profiles by applying collimation and anamorphic optics. Optimized output power is 20 mW for the signal laser and 30 mW, respectively, for the pump laser, resulting in a maximum MIR optical power of approximately 30 nW. The MIR radiation is generated in a 30 mm $AgGaS_2$ crystal via noncritical 90° type I phase matching after polarization adjustment and spatial overlapping of the two beams. Thereby, a frequency conversion efficiency of 0.06 mW W^{-2} cm^{-1} was obtained. By frequency tuning of the signal laser and varying the temperature of the crystal, the wavelength of the MIR radiation can be tuned from 4.9 to 5.1 µm. Operation parameters were set according to the CO P(28) transition at 4.94 µm wavelength. The spectral resolution of the system is determined by an output linewidth of $1.2 \cdot 10^{-2}$ cm^{-1} and a scanning range of 1.2 cm^{-1}/V. With a voltage ramp of 5 V at the signal laser, a total spectral range of 6 cm^{-1} (approximately 15 nm around 4.9 µm wavelength) can be covered in one scan. Important properties of the spectroscopic source and operation parameters are summarized in table 1.

Table 1. Output characteristics and operation parameters of the MIR DFG laser system considered

output characteristics:	
continuous MIR optical output power in nW	30
conversion efficiency in mW W^{-2} cm^{-1}	0.06
linewidth in cm^{-1}	$1.2 \cdot 10^{-2}$
centre wavelength in µm	4.94
centre wavelength in cm^{-1}	2023
scanning range in cm^{-1} V^{-1}	1.2
operation parameters:	
crystal temperature in °C	30.6 ± 0.1
signal laser temperature in °C	30.0 ± 0.01
pump laser temperature in °C	15.0 ± 0.01
signal laser current in mW	98.4
pump laser current in mW	70.4
signal laser voltage ramp in V	5.0

The laser system was put into a water cooled aluminium box of the size (70x75x30) cm^3 as shown in figure 2. A stable temperature of 28 °C was achieved within the box. Thus, the crystal temperature could be stabilized around 30.6 °C by heating elements to meet the phase matching condition. Thermal stabilization of the lasers was done with Peltier elements at temperatures between 10 and 40 °C, heat sink being water. The effect of crystal temperature as well as

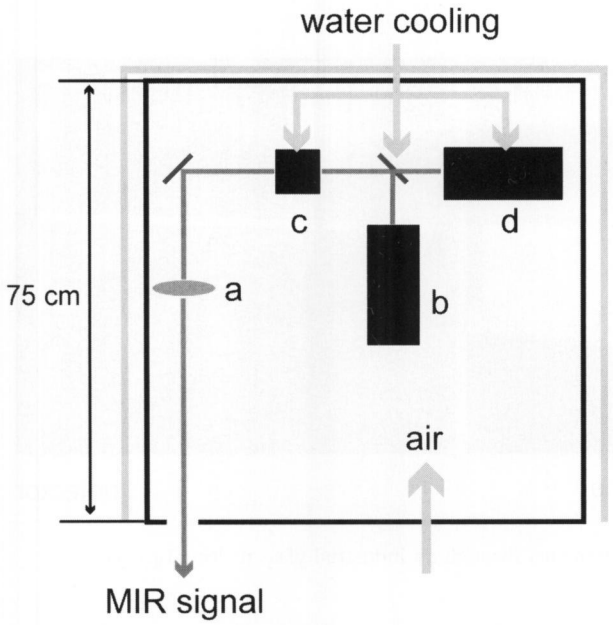

Figure 2. Aluminium box with laser system for industrial application (a: CaF_2 lens, b, d: diode laser with collimation and anamorphic optics, c: $AgGaS_2$ crystal).

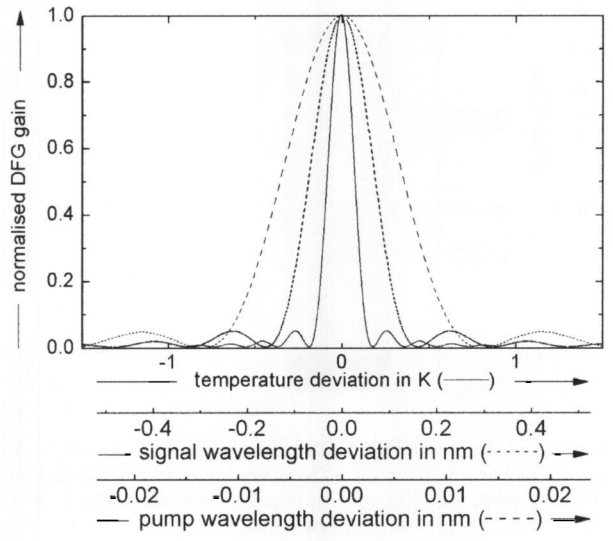

Figure 3. Acceptance curves of the DFG-system: normalized DFG gain versus temperature and input wavelength deviation.

signal and pump wavelength instabilities are illustrated in figure 3, providing the calculated behaviour of MIR DFG gain dependent on parameter deviations. It underlines the need for accurate parameter adjustment and temperature control.

2.2 Detector

For signal detection, a photovoltaic InSb detector with an active area of 1 mm^2 was used. A band pass filter with a centre wavelength at 4.87 µm and a halfwidth of 0.216 µm as well as an additional germanium plate in front of the

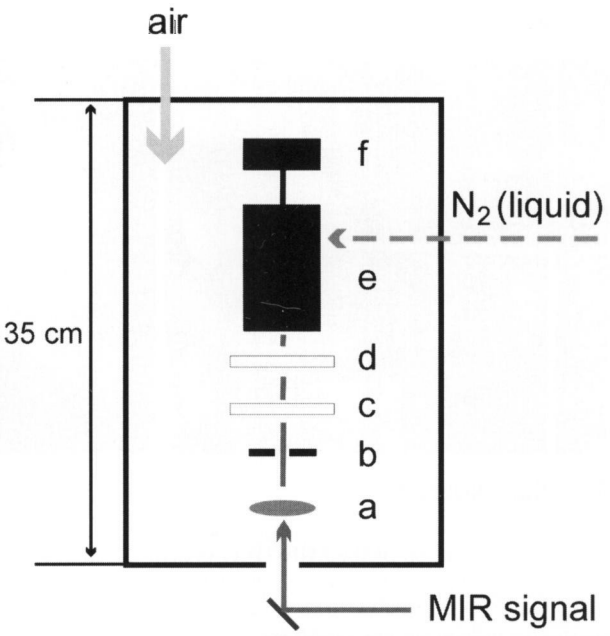

Figure 4. Aluminium box with detector for industrial application (a: CaF_2 lens, b: diaphragm, c: Ge filter, d: bandpass filter, e: detector, f: pre-amplifier).

Table 2. Commercial elements used for the spectrometer

signal laser	Sharp LT024MDO diode & controller, 787 to 791 nm
pump laser	Toshiba TOLD 9150 diode & controller, 680 to 682 nm
thermo-stabilization	Peltier (Marlow MI1063-T), copper
detector	Polytec R-1730 IS, pre-amplifier DP 8100 A
filter	cut-off: germanium, 1 mm thick bandpass: centre 4.875 µm, halfwidth 0.216 µm
amplifier	lock-in (EG & G 5210), mechanical chopper (HMS 230)
NLO medium	$AgGaS_2$, (30 x 4 x 4) mm^3
beam guidance, collimation and shaping	CaF_2 lenses, collimator, anamorphot (Schaefter & Kirchhoff)

detector are applied to cut off disturbing background radiation. CaF_2 lenses and silver mirrors are used for guiding and imaging of the MIR beam. The output signal of the detector is processed with a lock-in amplifier in conjunction with amplitude modulation of the MIR radiation applying a mechanical chopper. The typical carbon monoxide detection limit obtained with this setup is around 5 ppm · m [9]. Detector and pre-amplifier were put into an aluminium box of the size (50x40x40) cm^3 to protect them from the harsh environment (figure 4). The detector is cryogenically cooled, using 100 ml/h liquid nitrogen.

The most important components applied to the spectrometer are listed in table 2.

2.3 Optical path

For a coarse adjustment of the optical path through the furnace a green HeNe pilot laser was employed. The red

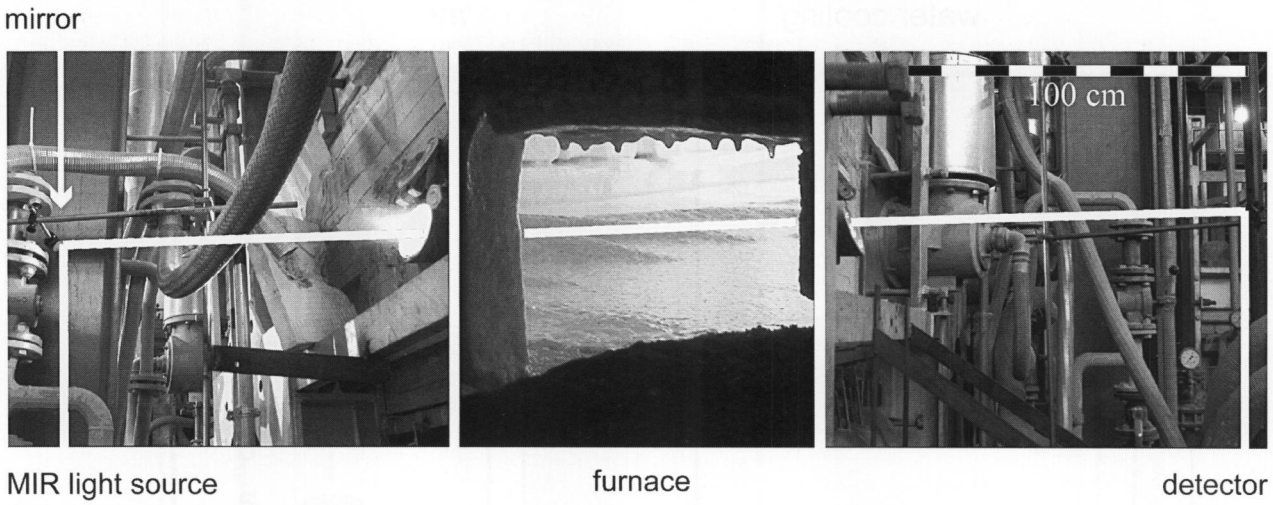

Figure 5. Application of the MIR-DFG system for cross-duct measurements through an industrial glass melting furnace.

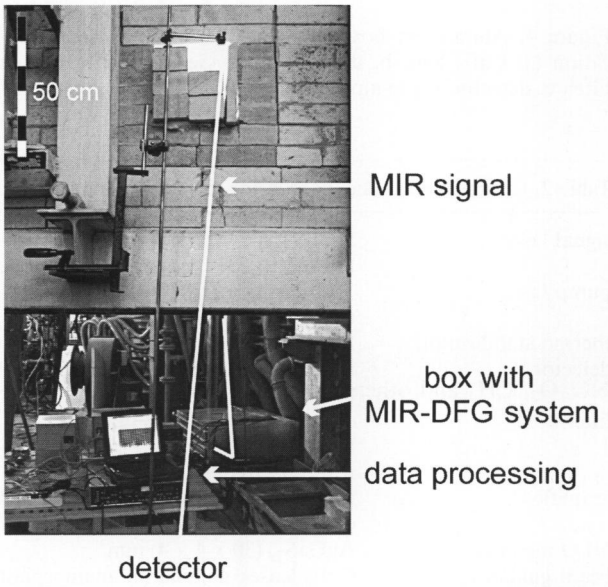

Figure 6. CO detection at the recuperator of an industrial glass melting furnace.

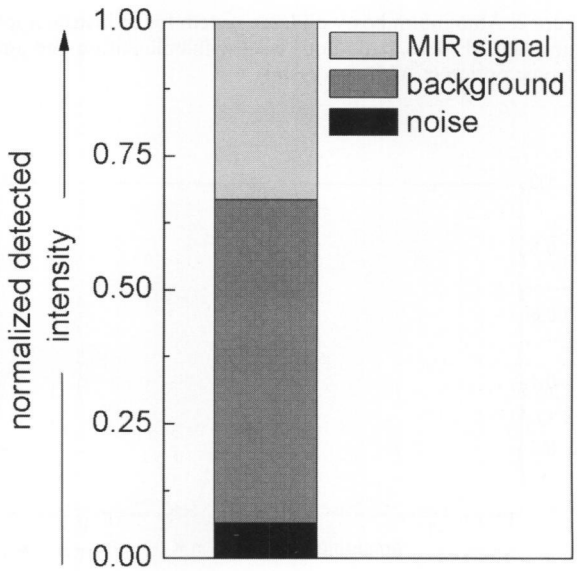

Figure 7. Comparision of transmitted MIR laser signal, background radiation and noise as measured at constant wavelength (4.9 μm) while crossing the furnace at approximately 1500 °C and a "hot" absorption path of 350 cm.

signal laser beam was then with this laser, assuming that signal laser and invisible MIR laser coincide. The detector and laser boxes were installed on the steel frame of the furnace to minimize mechanical vibration and mirrors were used to guide the beam.

Two arrangements were applied to the absorption experiments:

a) directly through the furnace at a height of approximately 30 cm above the glass melt and crossing the flame of one of the side burners. In this case, the pathlength through the hot furnace atmosphere (approximately 1500 °C) was about 380 cm, which results in a total optical pathlength (including beam guidance outside the furnace) of about 800 cm (figure 5), and

b) as shown in figure 6 through the entry of the recuperator channel, crossing 100 cm at T >1100 °C and a total pathlength of 550 cm.

Adjustment and optical fine tuning of the DFG system were done on site. A system check was performed at the final position of the spectrometer by measurements through a reference cell containing CO.

3. Results and discussion

At first view, inherently low frequency conversion efficiency and therefore low MIR gain seem to be a main drawback of nonlinear optics for spectroscopic sources in industrial applications. On the other hand, an initial signal of an optical output power as low as 30 nW can still be detected after crossing the extremely harsh environment of a gas fired industrial glass melting furnace (figure 7). That is especially

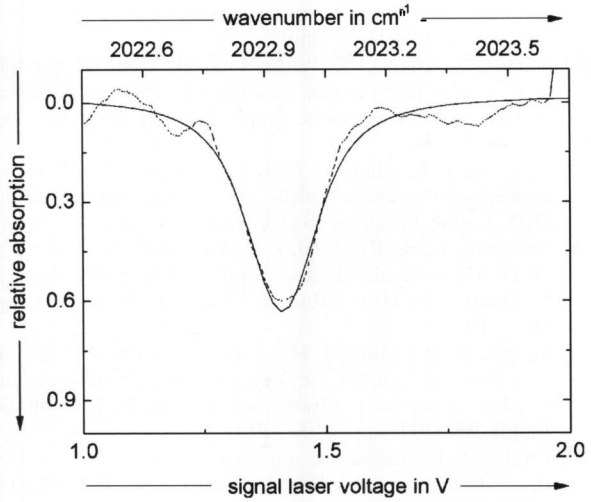

Figure 8. CO absorption measured in the recuperator at approximately 1100 °C over a "hot" absorption path of 100 cm.

Table 3. Experimentally determined line broadening coefficients as used for data quantification (CO P(26) at 25 °C)

	α in $cm^{-1} \cdot bar^{-1}$
CO–Ar	0.030 ± 0.001
CO–CH_4	0.093[1] ± 0.0151
CO–CO	0.056 ± 0.003
CO–CO_2	0.020 ± 0.001
CO–H_2O	0.104[2] [10]
CO–N_2	0.033 ± 0.002
CO–O_2	0.027 ± 0.002

[1] CO P(28)
[2] CO P(27)

due to the possibility of highly selective filtering and modulation techniques. However, as the intensity of background radiation and noise is still about twice as high as that of the detectable MIR laser signal for measurements directly through the furnace, one has either to enhance MIR power or to alleviate measuring conditions. This was done by shortening the length of the "hot" absorption path and measuring in colder areas of the furnace. Therefore, further measurements were performed at the hot end of the recuperator channel of the furnace as mentioned before.

In figure 8, the averaged and background corrected absorption spectrum of 12 measurements near 4.94 µm (2023 cm^{-1}) over a time of 20 min is illustrated. The absorption peak corresponds to the CO P(28) line at 2022.9 cm^{-1}. Assuming binary line broadening coefficients as given in table 3 [8] and an atmospheric composition around [H_2O] = 20 vol.%, [CO_2] = 13 vol.%, [O_2] = 1 vol.% and [N_2] = 65 vol.%, for a temperature of 1100 °C and a pressure of 1 bar, data evaluation as described in [1] yields a CO concentration of 400 ppm (500 mg/m^3). Spectroscopic data was adopted from the HITRAN database [11]. At this point, the accuracy of the method is determined mainly by background and baseline correction techniques, which is due to low absolute MIR intensity. The estimated error is 15 % and is expected to significantly decrease with increasing MIR intensity. Therefore, the authors are working on MIR intensity enhancement by fiber and semiconductor amplifiers. First results indicate an amplification of signal and pump laser by at least a factor of 20, which yields MIR output power in the µW range (equation 3).

The detected signal is strongly affected by beam steering due to optical turbulences and dust within the furnace [12 and 13]. Regarding the relatively long absorption path and maximum temperature changes of some 100 K, steering due to refraction and scattering is to be expected in the range of some mm, which is well beyond the beam diameter. In fact, during measurements through the furnace and burner flames, beam deflection and widening up to 5 cm occurs. Thus, accurate re-focussing of the signal after passing the furnace is an essential requirement.

On the other hand, mechanical vibrations and high environmental temperatures seem to be uncritical for operation and accuracy of the spectrometer and peripheral electronics over a measuring time of five days. This clearly underlines the suitability of the device for application in the glass industry.

4. Conclusions

The feasibility of an open-path DFG based mid-infrared spectrometer for in situ combustion monitoring in the glass industry has been demonstrated for the first time. Compared to probing techniques or extractive flue gas analysis, it offers several advantages: it operates overall contact-free and allows high temporal resolution, enhanced sensititvity and selectivity. It is applicable to the detection of a large number of combustion species, aside from CO also SO_2, NO, O_2, CH_4 and others, which illustrates the high versatility of the method. In conjunction with multiplexing, MIR LIDAR and other techniques that are rapidly emerging also simultaneous multi-species detection and three-dimensional resolution might be possible for industrial application within the next years. A drawback of DFG based devices is their inherently low MIR gain. That results in the requirement of novel amplifying techniques. However, recent work indicates the overcoming of this problem [14].

The main difficulty during cross-duct measurements turns out to be beam steering due to optical turbulences and scattering within the furnace. Careful beam guidance and focussing are required to achieve a stable signal. On the other hand, the influence of high temperature and mechanical vibration within the surrounding environment can be compensated with low effort.

*

These investigations were conducted with the kind support of the Arbeitsgemeinschaft industrieller Forschungsvereinigungen (AiF), Köln, (AiF-No. 13006 N) under the auspices of the Hüttentechnische Vereinigung der Deutschen Glasindustrie (HVG), Offenbach/M., utilizing resources provided by the Bundesminister für Wirtschaft und Arbeit, Berlin. Thanks are due to all these institutions.

Furthermore, we wish to thank the Dr. Genthe GmbH Co. KG, Goslar (Germany), for enabling measurements under industrial conditions.

5. References

[1] Wondraczek, L.; Khorsandi, A.; Willer, U. et al.: Mid-infrared laser absorption spectroscopy for process and emission control in the glass melting industry. Pt 1: Potentials. Glass Sci. Technol. **77** (2004) pp. 68-76.

[2] Schade, W.; Willer, U.; Wondraczek, L.: Mid-infrared laser sensors for mapping environment and combustions. Glass Sci. Technol. **76 C2** (2003) pp. 109–114.

[3] Boyd, R. W.: Nonlinear optics. Boston: Academic Press, 1992.

[4] Zondy, J. J.: The effects of focusing in type-I and type-II difference-frequency generation. Opt. Commun. **149** (1998) pp. 181–206.

[5] Chen, W.; Boucher, D.; Tittel, F. K.: Recent advances in continuous-wave laser difference-frequency generation in the mid-infrared: State of the art, applications, and perspectives. Recent Res. Devel. Appl. Phys. **5** (2002) pp. 27–68.

[6] Meschede, D.: Optik, Licht und Laser. Stuttgart et al.: Teubner, 1999.

[7] Willer, U.; Blanke, T.; Schade, W.: Difference frequency generation in $AgGaS_2$: Sellmeier and temperature-dispersion equations. Appl. Opt. **40** (2001) pp. 5439–5445.

[8] Wondraczek, L.; Khorsandi, A.; Willer, U. et al.: Mid-infrared laser-tomographic imaging of carbon monoxide in-laminar flames by difference frequency generation. Combust. Flame (2004). In print.

[9] Schade, W.; Blanke, T.; Willer, U. et al.: Compact tunable mid-infrared laser source by difference frequency generation of two diode-lasers. Appl. Phys. B **63** (1996) pp. 99–102.

[10] Varghese, P. L.; Hanson, R. K.: Room temperature measurements of collison widths of CO lines broadened by H_2O. J. Mol. Spectros. **88** (1981) pp. 234–235.

[11] Rothman, L. S.; Rinsland, C.P.; Goldman, A. et al.: The HITRAN molecular database and HAWKS: 1996 Edition. J. Quant. Spectros. Radiat. Transfer **60** (1998) pp. 665–710.

[12] Skaggs, R. R.; Miller, J. H.: A study of carbon-monoxide in a series of laminar ethylene air diffusion flames using tunable diode-laser absorption-spectroscopy. Combust. Flame **100** (1995) pp. 430–439.

[13] Ciddor, P. E.: Refractive index of air: New equations for the visible and near infrared. Appl. Optics **35** (1996) pp. 1566–1573.

[14] Liem, A.; Limpert, J.; Schreiber, T. et al.: High power fiber laser and amplifier systems. Glass Sci. Technol. **75 C1** (2002) pp. 211–222.

~ E304P005

Contact:

Dr.-Ing. Lothar Wondraczek
Institut für Nichtmetallische Werkstoffe
Technische Universität Clausthal
Zehntnerstrasse 2A
D-38678 Clausthal-Zellerfeld

E-mail: lothar.wondraczek@tu-clausthal.de